Chapter 3

Mixed monolayers of cholesteric acid and lipid molecules

3.1 Introduction

The studies on Langmuir monolayer of cholesteric acid (ChA) at the air-water (A-W) interface show many interesting results. We have observed different two-dimensional (2D) phases like $L_1^{'}$, $L_2^{'}$ and L_2. In this chapter, we describe our studies on the stability of the phases and miscibility of binary mixture of ChA and lipid molecules of different structures. We have chosen the lipid molecules like cholesterol (Ch), stearic acid (SA) and L-α-dipalmitoyl phosphatidylcholine (DPPC).

Lipids are important constituents of the biological membranes. They have a broad classification which primarily includes the phopholipids, fatty acids and sterols (cholesterol, ergosterol, dehydrocholsterol). Fatty acids are known to regulate the blood pressure [1]. They also reduce the risk of hypercholesterolemia by lowering the level of low density lipoprotein-bound cholesterol [2]. Stearic acid (a fatty acid) possesses a linear alkyl chain with a carboxylic head group. Phopholipids are the main constituents of the lung surfactant. The phospholipids monolayers mimic the biological membranes and have been extensively studied [3]. DPPC (a phospholipid) is one of the most commonly studied compound. It has two aliphatic tails and a bulkier phosphocholine head group. The phosphocholine head group acquires a large value of dipole moment in the polar solvent like water. It is interesting to study the 2D miscibility of the ChA with lipid molecules of different structures like Ch,

SA and DPPC.

3.2 Experimental

Cholesterol (Ch) was procured from Aldrich and was recrystallized twice in ethanol solvent. Stearic acid (SA) was obtained from Aldrich and L-α-dipalmitoyl phosphatidylcholine (DPPC) was from Sigma. The solutions of the samples having a concentration of 1.94 mM were prepared in HPLC grade chloroform and the binary mixtures were prepared by mixing them in appropriate quantities. The chemical structures of the molecules are shown in Figure 3.1. The experimental details for surface manometry, Brewster angle and epifluorescence microscopy were similar as described in the previous chapters.

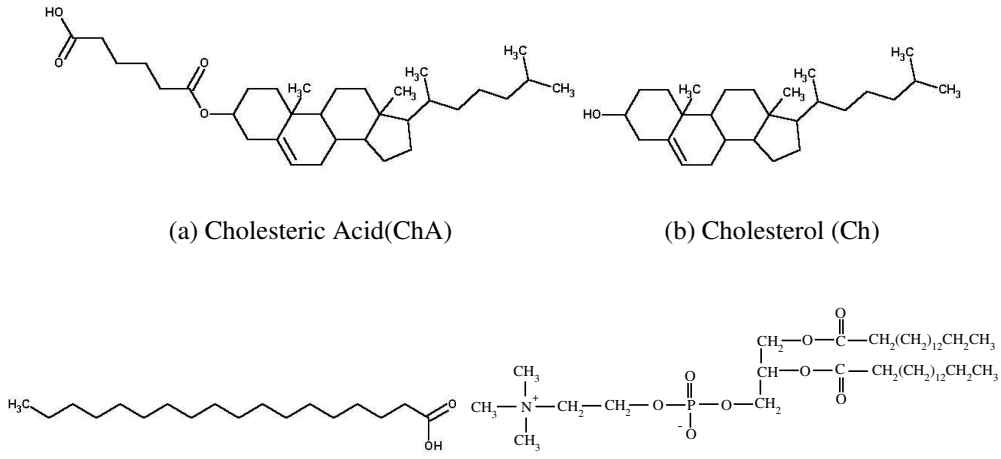

(a) Cholesteric Acid(ChA) (b) Cholesterol (Ch)

(c) Stearic Acid (SA) (d) L-α-Dipalmitoyl Phosphatidylcholine (DPPC)

Figure 3.1: Chemical structure of the molecules.

3.3 Results and Discussion

3.3.1 Mixed monolayer of cholesteric acid and cholesterol

The surface pressure (π) - area per molecule (A_m) isotherms for different mole fractions of Ch in the mixed monolayer of ChA and Ch (X_{Ch}) are shown in Figure 3.2. The ChA monolayer at the A-W interface exhibits a liquid phase with tilt-azimuth variation in the molecules (L_1'

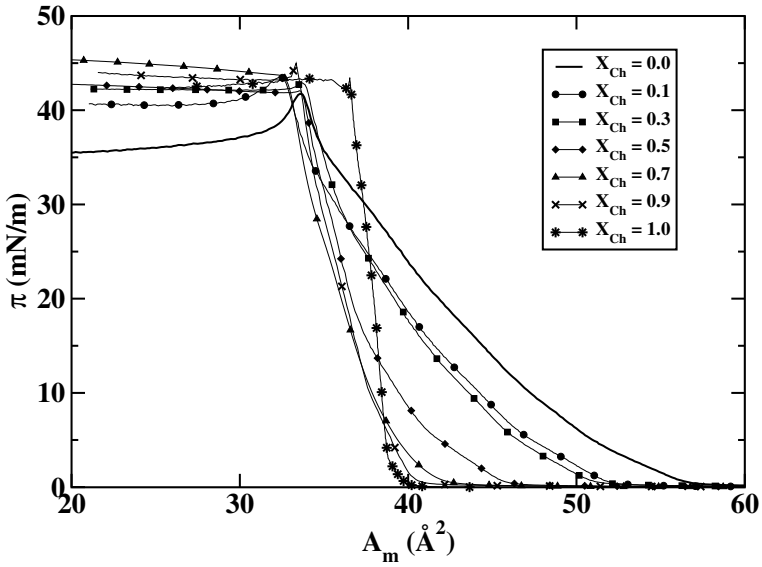

Figure 3.2: The surface pressure (π)-area per molecule (A_m) isotherms of the mixed monolayer for different mole fractions of Ch in ChA (X_{Ch}).

phase), liquid phase with uniformly tilted molecules ($L_2^{'}$ phase) and untilted condensed (L_2) phase. The monolayer of cholesterol (Ch) at the A-W interface shows a gas and an untilted condensed (L_2) phase [4]. The isotherms of the mixed monolayer corresponding to X_{Ch} equal to 0.1, 0.3 and 0.5 show a trend similar to that of pure ChA monolayer. They show three kinks representing three phases. However, the isotherms indicate a shift in the lift-off area per molecule (A_i) to the lower values with increasing X_{Ch}. The isotherms of the monolayers for higher mole fractions ($X_{Ch} > 0.5$) indicate the suppression of one of the phases, and they reveal two kinks indicating two phases. The extent of the steep region of the isotherms increases with increasing X_{Ch}. The collapse pressures of pure ChA and Ch have the values of 41.5 and 43 mN/m, respectively. The collapse pressures of the mixed monolayer as a function of mole fraction remains nearly the same. Table 3.1 shows the limiting area per

X_{Ch}	0.0	0.1	0.3	0.5	0.7	0.9	1.0
A_o (Å^2)	40.8	39.6	39.6	39.3	37.0	37.4	39.0

Table 3.1: The limiting area per molecule (A_o) determined from the isotherms shown in Figure 3.2.

molecule (A_o) values for the isotherms shown in Figure 3.2. The A_o values do not show much variations with X_{Ch}. This is due to similar cross-sectional area of both the molecules. The A_o values suggest that the molecules may be orienting normal to the interface in the

condensed phase.

The phases of the two-component monolayer system were investigated using Brewster angle and epifluorescence microscopy. In the previous chapter, which deals with the study of pure ChA monolayer, we find interesting stripe patterns in the BAM images of $L_1^{'}$ phase. However, the $L_2^{'}$ and L_2 phases show an uniform texture in BAM and the epifluorescence images. Similarly, the pure Ch monolayer shows an uniform texture for the L_2 phase in the microscopy imaging [5]. The BAM images of the mixed monolayer for different X_{Ch} are shown in Figure 3.3. The characteristic stripe pattern of the $L_1^{'}$ phase was seen to exist in the BAM images of the mixed monolayer having the compositions upto X_{Ch} equal to 0.5. Figure 3.3(a) shows the stripe pattern for X_{Ch} equal to 0.3. The features tend to weaken with increasing X_{Ch}. The BAM image for X_{Ch} equal to 0.5 (Figure 3.3(b)) shows faint and large stripes. For X_{Ch} value greater than 0.5, the BAM images of the monolayer do not reveal the stripe pattern, and it shows only an uniform gray texture. This can be seen from the BAM image of the monolayer of X_{Ch} equal to 0.7 (Figure 3.3(c)) which shows an uniform texture at a large A_m. The BAM images in the other phases of the mixed monolayer show uniform textures. Figure 3.4 shows a BAM image captured in the steep region of the isotherm corresponding to X_{Ch} equal to 0.5. Here the image shows only an uniform texture. The collapsed state of the mixed monolayer shows bright 3D domains coexisting with a condensed phase.

We have studied the mixed monolayer of ChA and Ch using the epifluorescence microscopy for different X_{Ch}. We find gas (dark region) and the liquid domains (gray domains) at large A_m (Figure 3.5(a)). Compression of the monolayer yielded a very uniform gray texture indicating an uniform phase (Figure 3.5(b)). Similar behavior was seen for all the compositions. Compression of the mixed monolayer does not show any textural change other than uniform gray texture throughout the monolayer regime. The absence of stripe pattern during the low magnification epifluorescence imaging suggests that the patterns seen in the BAM images (Figure 3.3) are due to tilt-azimuth variation rather than surface density variation. In the BAM and epifluorescence microscope observations, we do not find a phase

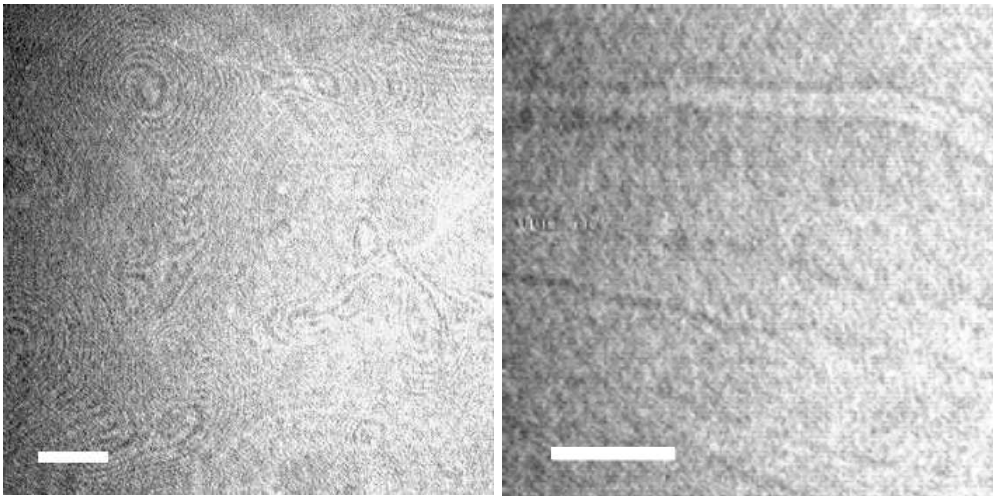

(a) X_{Ch} = 0.3, A_m = 50.0 Å^2

(b) X_{Ch} = 0.5, A_m = 45.3 Å^2

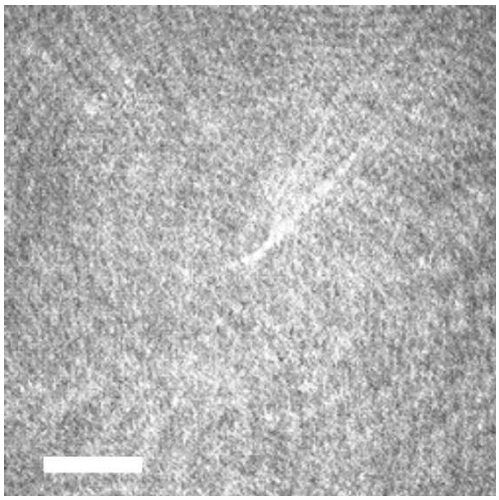

(c) X_{Ch} = 0.7, A_m = 41.0 Å^2

Figure 3.3: BAM images of the mixed monolayer for different mole fractions of Ch in ChA (X_{Ch}). The images were captured at an A_m shown below the respective images. (a) shows a stripe pattern, (b) shows faint and large stripes and (c) shows an uniform gray texture. The images show part of concentric ellipses in the background which are artifacts arising due to scattering of laser light from very fine dust particles on the lens and polarizer of the microscope. Such features appear prominently in the images with uniform background. The scale bar represents 500 μm.

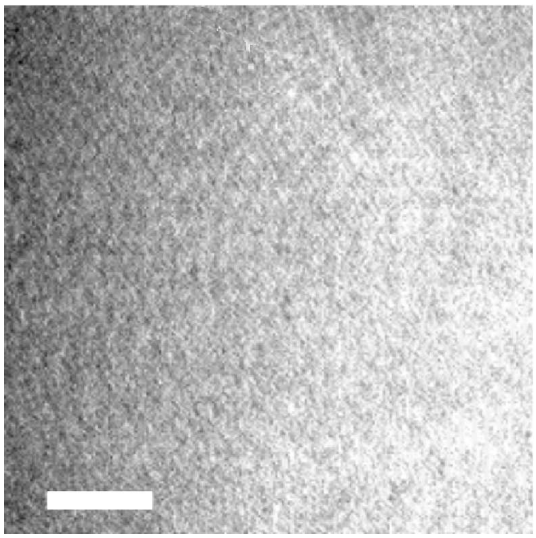

Figure 3.4: BAM image of the mixed monolayer for 0.5 mole fraction of Ch in ChA showing an uniform texture. The image was captured at the A_m of 36.6 Å^2. The image shows part of concentric ellipses in the background which are artifacts arising due to scattering of laser light from very fine dust particles on the lens and polarizer of the microscope. The scale bar represents 500 μm.

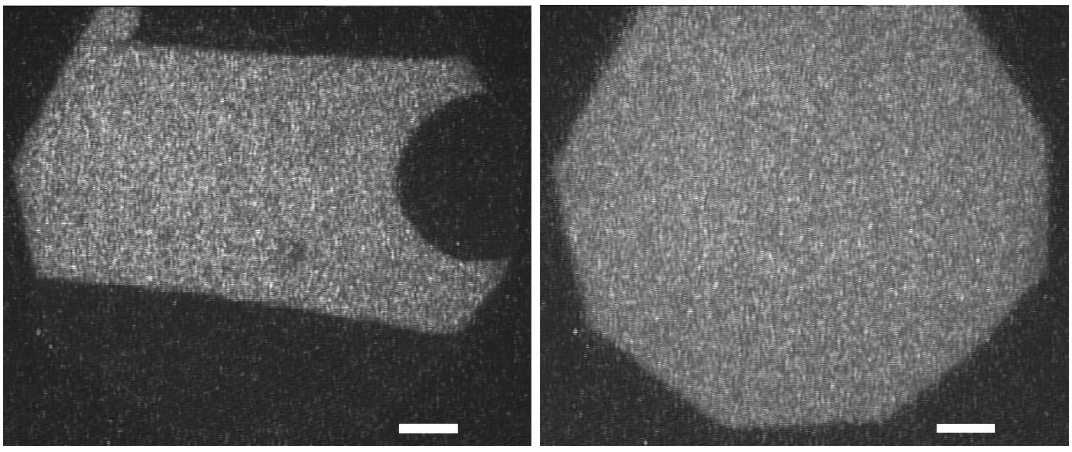

(a) A_m = 82.0 Å^2 (b) A_m = 40.0 Å^2

Figure 3.5: Epifluorescence images of the mixed monolayer for 0.5 mole fraction of Ch in ChA (X_{Ch}). The images were captured at an A_m shown below the respective images. (a) shows a coexistence of gas (dark region) and a liquid-like gray domains. (b) shows an uniform gray texture. The scale bar represents 50 μm.

separation of the two components (Ch and ChA) in the mixed monolayer systems. This indicates a miscible nature of the components in the mixed monolayer.

We have studied the time evolution of the stripe patterns observed during BAM imaging of the mixed monolayer for different compositions. The images captured at a time interval of five minutes are shown in Figure 3.6. The features get enhanced with increasing time. The

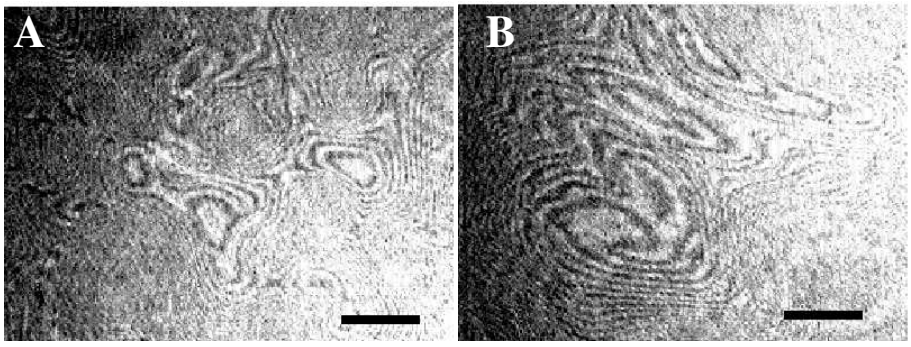

(a) X_{Ch} = 0.1

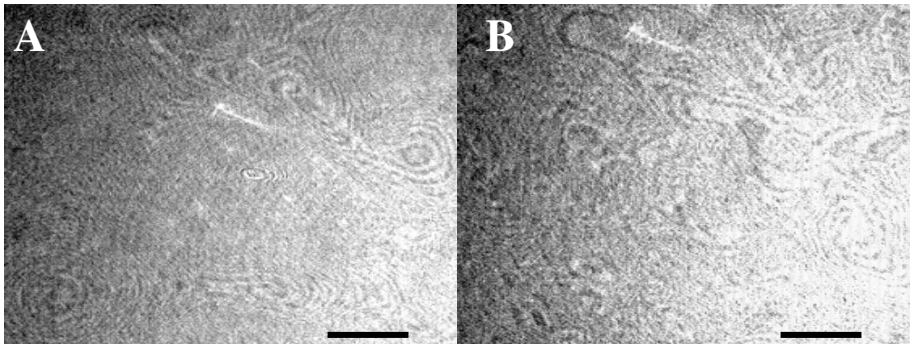

(b) X_{Ch} = 0.3

Figure 3.6: The temporal evolution of the patterns obtained during BAM imaging of the mixed monolayer of ChA and Ch. The compositions of the monolayer are shown below the respective images. The images were captured at 2.5 mN/m which corresponds to the $L_1^{'}$ phase of the pure ChA monolayer. The time difference between the images A and B are 5 minutes. The images show part of concentric ellipses in the background which are artifacts arising due to scattering of laser light from very fine dust particles on the lens and polarizer of the microscope. The scale bar represents 500 μm.

stripe patterns are distinctly seen in the monolayer for X_{Ch} equal to 0.1 and 0.3 (Figure 3.6(a) and (b)). The appearance of stripe patterns in the BAM images of the monolayer upto X_{Ch} equal to 0.5 indicates the existence of the $L_1^{'}$ phase. The corresponding isotherms (for X_{Ch}

≤0.5) also indicate a kink (in the surface pressure range of 4.5 - 5.5 mN/m) representing a phase transition from the L_1' phase to a condensed phase. For the higher value of X_{Ch}, the kink in the isotherms of the monolayer vanishes. For monolayer of composition with X_{Ch} values greater than 0.5, the BAM and epifluorescence images show only an uniform texture. This indicates a suppression of the L_1' phase at the higher compositions (X_{Ch} >0.5). On compressing the monolayer for the X_{Ch} between 0.1 and 0.5 beyond the A_m corresponding to the L_1' phase, the isotherms show a gradual rise in surface pressure. This region of the isotherms indicates a large value of extrapolated A_m. It is accounted for a tilt of the molecule in the monolayer. The BAM and epifluorescence images show an uniform gray texture in this region of the isotherms indicating an uniform tilt of the molecules. Hence, this region of the isotherm can be considered as L_2' phase. For X_{Ch} greater than 0.5, the isotherms show two regions; an initial gradual rise and then a steep rise in the surface pressure. The region corresponding to the gradual rise shows a large value of A_m. The microscope observations corresponding to this region of the isotherm reveal an uniform texture. Hence, this region may correspond to the L_2' phase. The BAM images in the steep region of the isotherms also show a very uniform texture indicating an uniform orientation of the molecules. The limiting area per molecule (A_o) suggests a normal orientation of the molecule. Hence, this region of the isotherms may correspond to the untilted condensed (L_2) phase.

The variations of the in-plane elastic modulus (E) as a function of A_m for different X_{Ch} are shown in Figure 3.7. For pure ChA monolayer, the variation of E shows a small peak at 56 Å^2 indicating a transition from the coexistence of L_1' and gas phases to the L_1' phase. The region corresponding to the L_2' phase shows fluctuations in E. A sharp increase in E at around 34.5 Å^2 indicates a transition to the L_2 phase. The peak value of E of ChA in the L_1' and L_2 phases were found to be around 50 and 175 mN/m, respectively. With increasing X_{Ch} (≤ 0.5), the peak value of E in L_1' phase remains invariant. For a composition X_{Ch} greater than 0.5, the peak corresponding to the L_1' phase vanishes indicating a suppression of L_1' phase. The peak value of E in the L_2 phase shows a systematic increase with the increase in the X_{Ch}. The variation of E for the pure Ch monolayer shows a very steep rise in the value

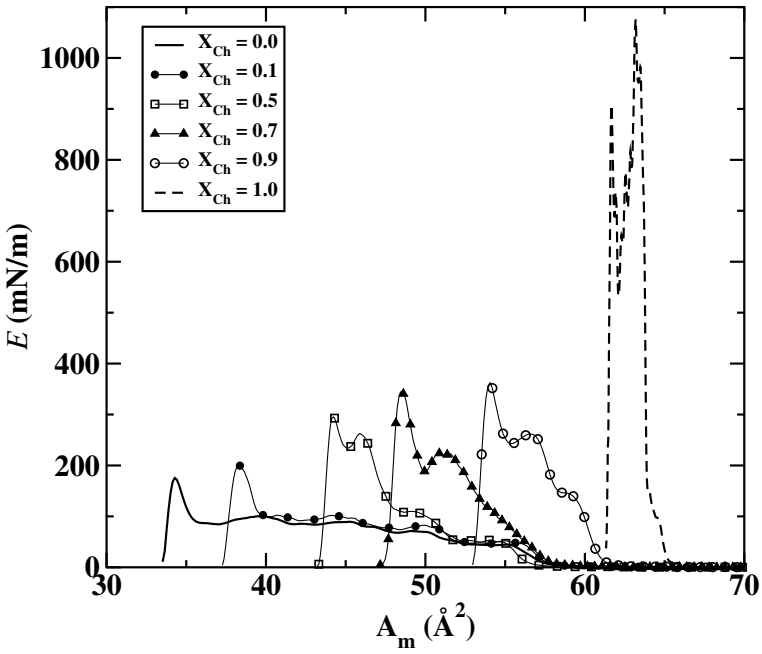

Figure 3.7: Variation of in-plane elastic modulus (E) as a function of A_m for different mole fractions of Ch in ChA (X_{Ch}). The data presented for the E are smoothened by taking a sliding window of five data points and performing a running average for three times. The curves (except for X_{Ch} = 0.0) are relatively shifted horizontally by 5 Å^2 for visual clarity.

at around 39 Å^2. This indicates a phase transition from a coexistence of gas and L_2 phases to the L_2 phase. The peak values of E of Ch in the L_2 phase was found to be 1076 mN/m at 38.5 Å^2. This is about 2.6 times greater than that of L_2 phase of the mixed monolayer for X_{Ch} equal to 0.9.

For an ideal case of complete miscibility or immiscibility of two-component monolayer system, the area of the mixed monolayer is given by the rule of additivity,

$$A_{id} = A_1X_1 + A_2X_2 \tag{3.1}$$

where X_1 and X_2 are the mole fractions of the components 1 and 2, respectively. A_1 and A_2 are the A_m of the individual pure component monolayers. However, for a mixed system, the monolayer area can deviate from the ideal case. Such deviation in the monolayer area depends on the nature of the interaction between the component molecules and is known as the excess area per molecule, A_{ex}. The A_{ex} is defined as

$$A_{ex} = A_{12} - A_{id} \tag{3.2}$$

where A_{12} is the experimentally determined values of the A_m of the mixed monolayer. A_{id} is the ideal A_m value calculated from Equation 3.1. The positive or the negative value of the A_{ex} indicates a repulsive or an attractive interaction, respectively between the component molecules in the mixed monolayer.

The excess area per molecule was calculated using Equation 3.2 for different X_{Ch} and at different surface pressures. The variation in A_{ex} as a function of X_{Ch} at different surface pressures (Figure 3.8) shows negative values for all the compositions. The negative values

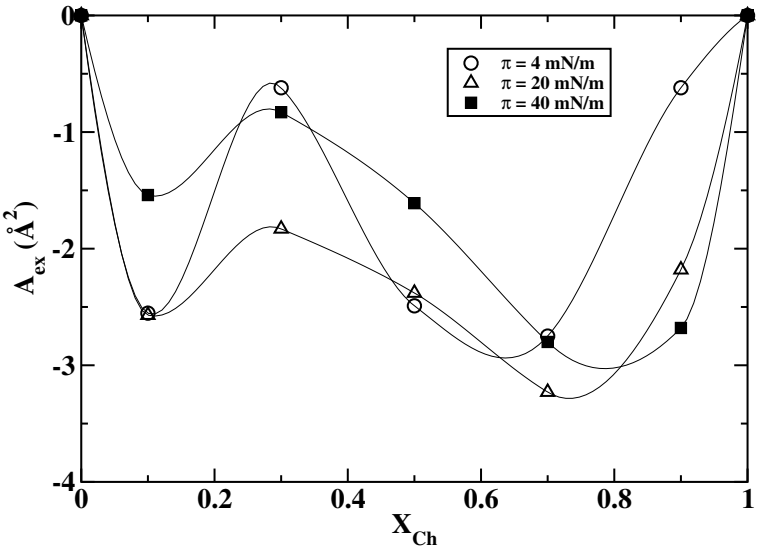

Figure 3.8: Excess area per molecule (A_{ex}) as a function of mole fraction of Ch in ChA (X_{Ch}) at different surface pressures (π). The points denote the calculated values obtained from the experimental data. They are joined by smooth lines.

of the A_{ex} (Figure 3.8) indicate an attractive interaction between the ChA and Ch molecules throughout the monolayer regime.

The stability and the degree of miscibility of a mixed monolayer were studied by calculating the excess Gibbs free energy (ΔG) [6, 7]. The ΔG is given by

$$\Delta G = N_a \int_0^{\pi} A_{ex} d\pi \tag{3.3}$$

where N_a is the Avogadro number and π is the surface pressure.

The variation of ΔG with respect to X_{Ch} at different surface pressures (Figure 3.9) shows negative values for all the compositions. It shows a minimum at around X_{Ch} equal to 0.7.

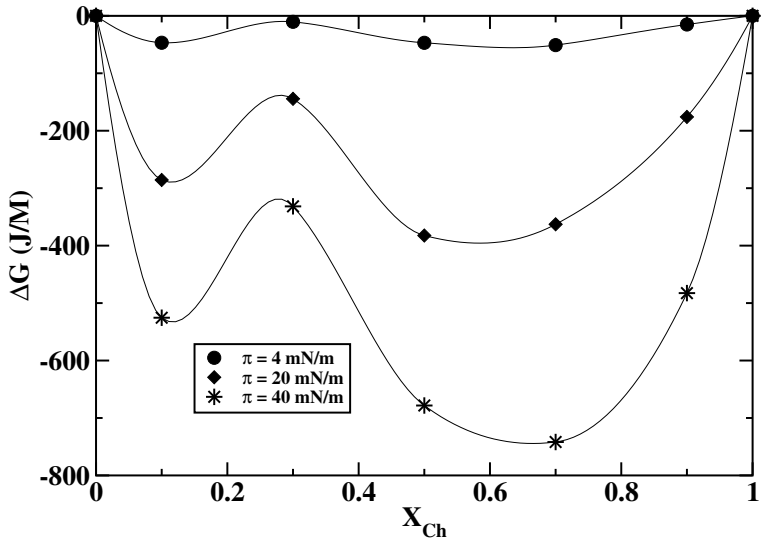

Figure 3.9: The excess Gibbs free energy (ΔG) as a function of mole fraction of Ch in ChA (X_{Ch}) at different surface pressures (π). The points denote the calculated values obtained from the experimental data. They are joined by smooth lines.

This suggests a miscible nature of the component molecules (*i. e.* ChA and Ch) in the mixed monolayer with the stable composition being at around X_{Ch} equal to 0.7.

The thermodynamical and the microscopy studies on the mixed monolayer of cholesteric acid and cholesterol suggest the monolayer to be miscible for all compositions. The ChA molecule is structurally similar to that of Ch possessing a similar sterol moiety. The attractive interaction between the ChA and Ch molecules in the mixed monolayer can arise due to the van der Waals and hydrophobic interactions between the sterol moiety. In the present case, the -COOH group of ChA can form hydrogen bond with water molecules in the similar way as that of -OH of Ch. Hence, the presence of Ch in ChA monolayer does not perturb the hydrogen bond network at the interface. This in turn may not change the overall entropy of the system [8]. Therefore, the miscibility of the ChA and Ch can be attributed to the attractive interaction between the sterol moiety and the ease of formation of hydrogen bond of -COOH with water and the neighboring -OH group of the Ch molecules.

Based on our surface manometry and microscopy studies, we construct a phase diagram of the mixed monolayer system, as shown in Figure 3.10.

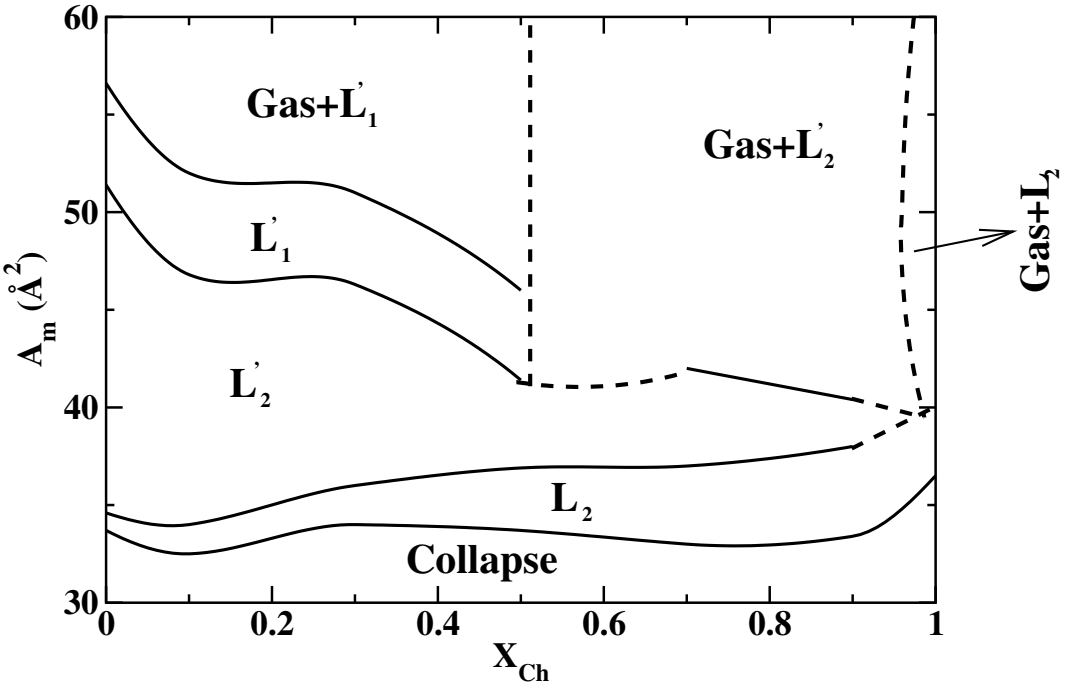

Figure 3.10: Phase diagram of the mixed monolayer system of cholestric acid (ChA) and cholesterol (Ch). X_{Ch} is the mole fraction of Ch in ChA and A_m is the area per molecule. The symbols $L_1^{'}$, $L_2^{'}$ and L_2 denote a liquid phase with tilt-azimuth varying molecules, a liquid phase with uniformly tilted molecules and untilted condensed phase, respectively. The solid lines are actual phase boundaries constructed from the experimental data points, whereas the dashed lines are the extrapolated phase boundaries.

3.3.2 Mixed monolayer of cholesteric acid and stearic acid

The Langmuir monolayer of cholesteric acid (ChA) mixed with stearic acid (SA) was studied using surface manometry and the microscopy experiments. Figure 3.11 shows the isotherms of the monolayer for different mole fractions of SA in ChA (X_{SA}). The SA monolayer is known to exhibit $L_{2_{SA}}^{'}$ and $L_{2_{SA}}$ phases [9]. In the $L_{2_{SA}}^{'}$ phase, the molecules are arranged on a distorted hexagonal lattice, and the tilt of the molecule is toward nearest neighbor. In $L_{2_{SA}}$ phase, the molecule stays normal to the interface on a regular hexagonal lattice. In the Figure 3.11, the isotherm of pure SA monolayer (X_{SA}=1.0) shows a coexistence of gas and $L_{2_{SA}}^{'}$ upto an A_m of 26 Å^2. In the region 26 to 20.5 Å^2, it exhibits $L_{2_{SA}}^{'}$ phase. In the region 20.5 to 20.0 Å^2, it shows the $L_{2_{SA}}$ phase [9]. In the mixed monolayer of ChA and SA, the isotherms shift systematically to the lower A_m with increase in X_{SA}. The extent of the steep region of the isotherms increases with increasing X_{SA}. The collapse surface pressures of the mixed

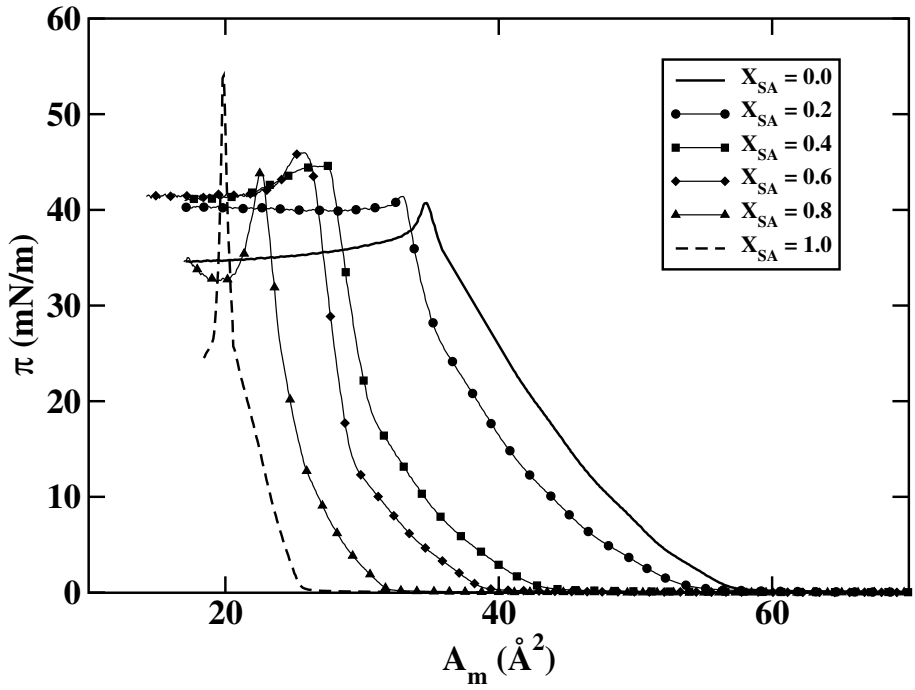

Figure 3.11: The surface pressure (π) - area per molecule (A_m) isotherms of the mixed monolayer for different mole fractions of SA in ChA (X_{SA}).

monolayer lie between that of the individual components. The A_o values obtained from the

X_{SA}	0.0	0.2	0.4	0.6	0.8	1.0
A_o (Å^2)	40.8	38.8	32.4	30.2	25.6	21.0

Table 3.2: The limiting area per molecule (A_o) determined from the isotherms shown in Figure 3.11.

isotherms (Figure 3.11) for various compositions are given in Table 3.2. The variation in the A_o was found to be linear with X_{SA}. The A_o values for different X_{SA} suggest a normal orientation of the molecules in the phase corresponding to the steep region of the isotherm.

The mixed monolayer for different X_{SA} was studied using the BAM and epifluorescence microscope. The BAM images of the mixed monolayer at different X_{SA} are shown in Figure 3.12. For X_{SA} equal to 0.2, the BAM image of the mixed monolayer shows a coexistence of gray and dark regions (gas phase) at a large A_m (Figure 3.12(a)). On compression, the dark region vanishes and the gray domains with a very weak stripe pattern were observed, as shown in Figure 3.13. On further compression, the stripe pattern vanishes, and the monolayer shows small bright domains in an uniform gray background (Figure 3.12(b)). The number of such bright domains increases on compression until the

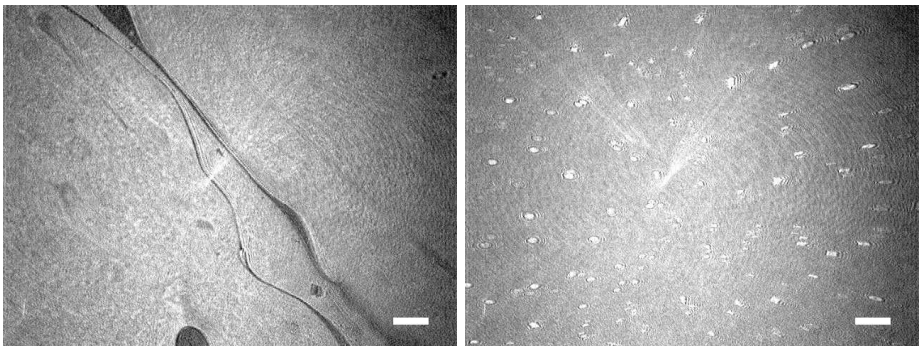

(a) X_{SA} = 0.2, A_m = 60.5 Å^2 (b) X_{SA} = 0.2, A_m = 40.0 Å^2

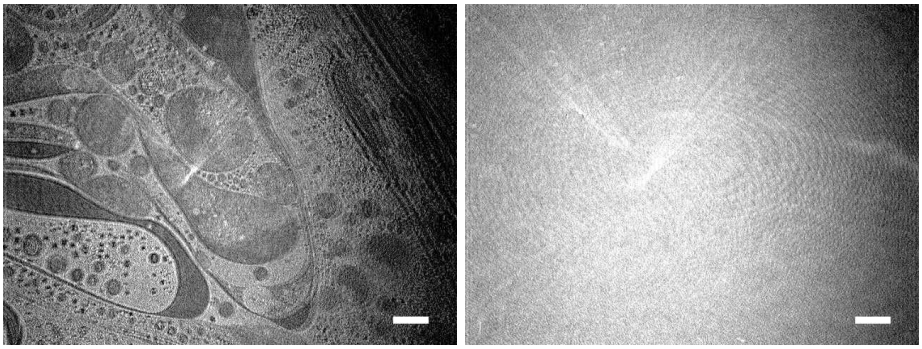

(c) X_{SA} = 0.4, A_m = 70.0 Å^2 (d) X_{SA} = 0.4, A_m = 33.3 Å^2

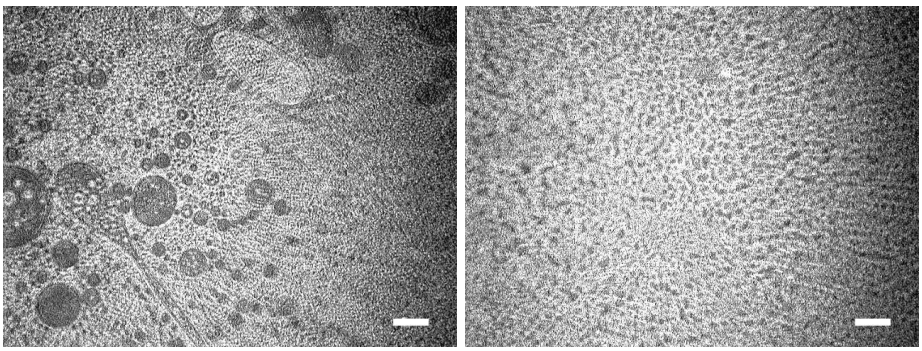

(e) X_{SA} = 0.8, A_m = 59.0 Å^2 (f) X_{SA} = 0.8, A_m = 31.7 Å^2

Figure 3.12: BAM images of the mixed monolayer for different mole fractions of SA in ChA (X_{SA}). The corresponding A_m and the X_{SA} values are shown below the respective images. (a) shows a coexistence of dark region (gas phase) and gray region. (b) shows small bright domains in an uniform gray background. (c) shows a coexistence of dark regions (gas phase) and gray domains. (d) represents an uniform gray region. (e) shows darker domains and dark spots embedded in gray domains. (f) reveals dark spots embedded in gray background. The scale bar represents 500 μm.

monolayer collapses. This indicates a phase separation. The BAM image of the monolayer for X_{SA} equal to 0.4 (Figure 3.12(c)) shows the coexistence of the gray domains and the dark regions (gas phase) at a large A_m. Compression of the monolayer leads to an uniform gray texture (Figure 3.12(d)). Further compression does not show any change in the texture. This indicates a miscibility of the mixed monolayer at X_{SA} equal to 0.4. The BAM images of the mixed monolayer for X_{SA} equal to 0.8 are shown in Figures 3.12(e and f). The image at large A_m shows a coexistence of darker domains (gas phase) and the gray region with embedded dark spots. On compression, the gas domains (darker region) vanish, and the more prominent embedded dark spots appear (Figure 3.12(f)). This indicates a phase separation.

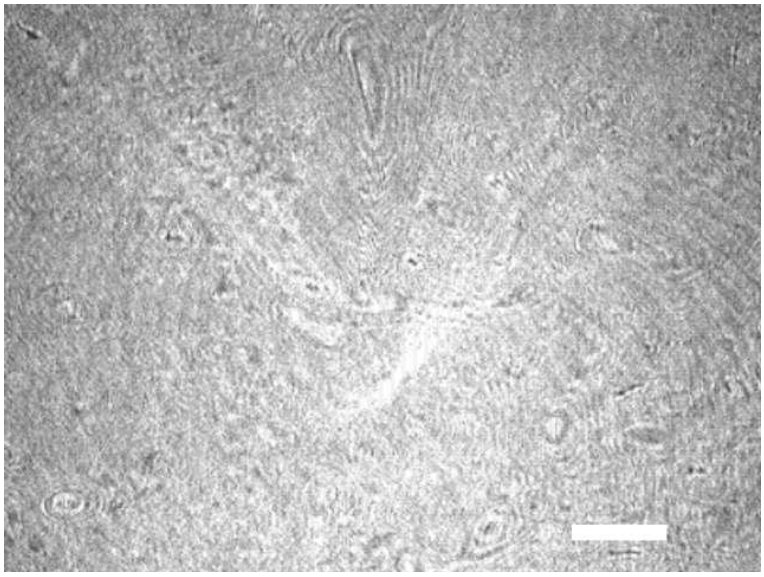

Figure 3.13: BAM image of a mixed monolayer for X_{SA} equal to 0.2 showing the stripe pattern of $L_1^{'}$ phase. The image was captured at an A_m of 50 $Å^2$. The image shows part of concentric ellipses in the background which are artifacts arising due to scattering of laser light from very fine dust particles on the lens and polarizer of the microscope. The scale bar represents 500 μm.

The epifluorescence images of the mixed monolayer for different X_{SA} are shown in Figure 3.14. The monolayer for X_{SA} equal to 0.2 displays the coexistence of a dark circular domain (gas phase) and the domains of two different gray levels at a large A_m (Figure 3.14(a)). On compression, the dark domains (gas phase) disappears. However, the domains corresponding to the two different gray levels continue to exist (Figure 3.14(b)) which indicates a phase separation. The ChA monolayer is more fluidic as compared to that

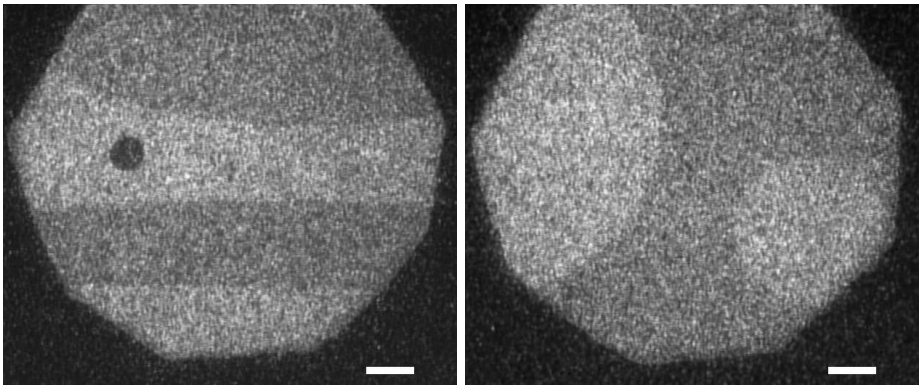

(a) X_{SA} = 0.2, A_m = 63.0 Å^2 (b) X_{SA} = 0.2, A_m = 40.0 Å^2

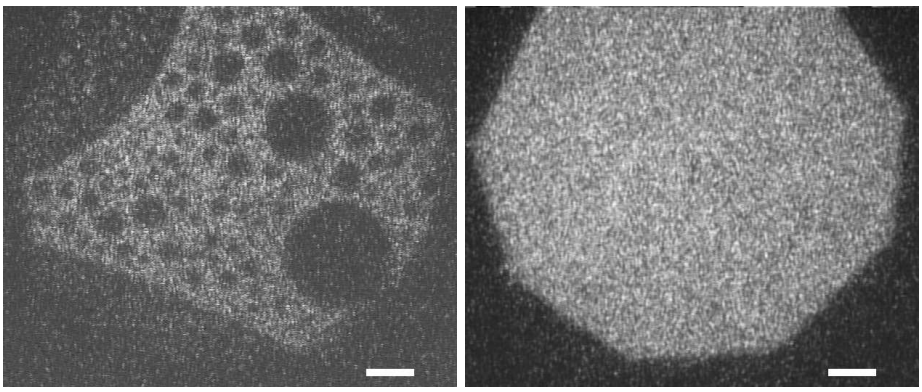

(c) X_{SA} = 0.4, A_m = 87.0 Å^2 (d) X_{SA} = 0.4, A_m = 35.0 Å^2

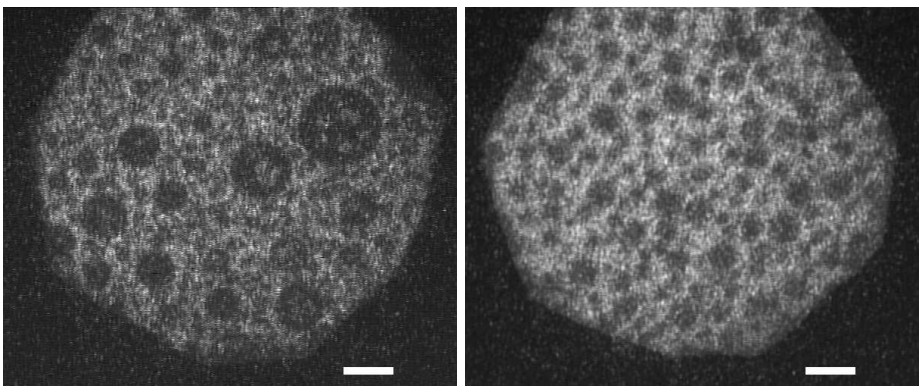

(e) X_{SA} = 0.8, A_m = 72.0 Å^2 (f) X_{SA} = 0.8, A_m = 26.5 Å^2

Figure 3.14: Epifluorescence images of the mixed monolayer for different mole fractions of SA in ChA (X_{SA}). The corresponding A_m and the X_{SA} values are shown below the respective images. (a) shows the coexistence of a dark circular domain (gas phase) and regions of two different intensity levels. Low intense domain represents a SA rich phase and the high intense region represents a ChA rich phase. (b) shows high intense domains (ChA rich phase) and low intense regions (SA rich phase). (c) shows dark region (gas phase) and gray domains. (d) shows a very uniform gray texture. (e) reveals dark region (gas phase) and embedded less intense gray spots in the more intense gray regions. (f) shows prominent less intense gray spots in more intense gray background. The scale bar represents 50 μm.

of SA as seen under the microscopes. Therefore, the miscibility of dye molecules in ChA rich domains is expected to be more as compared to the SA rich domains. This suggests that the less intense domains in the images may represent SA rich phase, whereas the more intense domains may represent ChA rich domains. The mixed monolayer for X_{SA} equal to 0.4 shows a coexistence of gas (dark domains) and a liquid like phase (gray region) at a large A_m (Figure 3.14(c)). Compression of the monolayer leads to an uniform gray texture (Figure 3.14(d)). At the higher concentration (X_{SA}=0.8) and at a large A_m (Figure 3.14(e)), a coexistence of the dark region (gas phase) and two gray levels are seen. On compression, the dark domains (gas phase) disappears and the less intense gray spots increase in size to appear prominently in the more intense gray background (Figure 3.14(f)). The less intense gray spots were seen to exist even in the steep region of the corresponding isotherm. The less intense gray spots may represent a SA rich phase, whereas the more intense gray region may represent a ChA rich phase. The results from the epifluorescence microscope experiments are consistent with those obtained from BAM results.

The isotherm corresponding to X_{SA} equal to 0.4 shows an initial gradual rise in surface pressure. Then there is steep rise in surface pressure. The region corresponding to the gradual rise shows a large value of extrapolated A_m which can be accounted by the tilt of the molecules in the monolayer. The BAM and epifluorescence images in this region of the isotherm show a very uniform texture indicating an uniform tilt of the molecules in the monolayer. Hence, this region of the isotherm may represent the $L_2^{'}$ phase. The BAM and epifluorescence images in the steep region of the isotherm also show a very uniform texture. This region of the isotherm may represent an untilted condensed (L_2) phase.

We have computed the excess Gibbs free energy (ΔG) of the mixed monolayer for different X_{SA} and at different surface pressures using Equation 3.3. The variations of ΔG with X_{SA} at different surface pressures are shown in Figure 3.15. The variation of ΔG shows the positive values at around X_{SA} equal to 0.2. This indicates the monolayer is unstable at this composition. The curves show a minimum negative value at around X_{SA} equal to 0.4. The values at the higher concentrations do not vary much and are comparatively small.

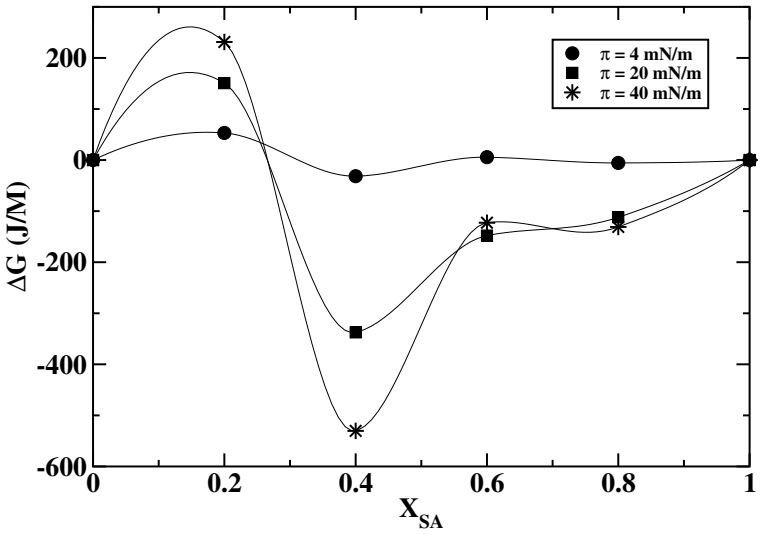

Figure 3.15: The variation of excess Gibbs free energy (ΔG) with respect to the mole fraction of SA in ChA (X_{SA}) at different surface pressures (π). The points denote the calculated values obtained from the experimental data. They are joined by smooth line.

The variation in ΔG indicates that X_{SA} equal to 0.4 is the stable composition of the mixed monolayer. This is consistent with the microscopy observations. Reports in literature suggest that a linear molecule (SA) is immiscible in a monolayer of sterol possessing molecule (Ch) [7]. Our system of the mixed monolayer of ChA and SA shows a better miscibility at around X_{SA} equal to 0.4. However, it shows immiscibility at other compositions.

Based on our surface manometry and microscopy study, we have constructed a phase diagram shown in Figure 3.16.

3.3.3 Mixed monolayer of cholesteric acid and DPPC

The L-α-dipalmitoyl phosphatidylcholine (DPPC) monolayer shows gas, liquid expanded (L_1'') and liquid condensed phases. In the liquid condensed phase, the tails of the molecules are uniformly tilted (~30°). The tilt angle reduces continuously on compression without changing the volume density leading to an untilted condensed phase [3]. Hence, the liquid condensed phase of DPPC can be designated as L_2 phase. The first order transition from L_1'' to L_2 phase is accompanied by a well defined coexistence of the phases.

In this section we discuss the study on the mixed monolayer of cholesteric acid (ChA) and DPPC. The surface pressure (π) - area per molecule (A_m) isotherms of the mixed monolayer

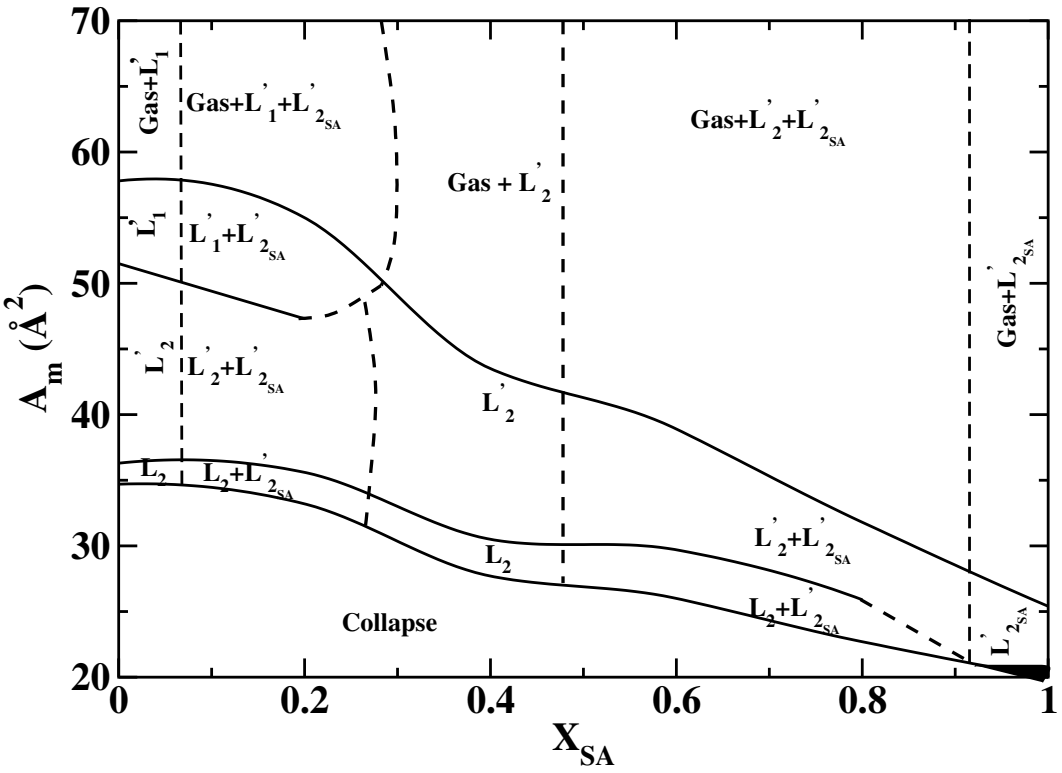

Figure 3.16: Phase diagram of the mixed monolayer of cholesteric acid (ChA) and stearic acid (SA). X_{SA} is the mole fraction of SA in ChA and A_m is the area per molecule. The symbols $L_1^{'}$, $L_2^{'}$, L_2, $L_{2_{SA}}^{'}$ and $L_{2_{SA}}$ denote a liquid phase with tilt-azimuth varying molecules, a liquid phase with uniformly tilted molecules, untilted condensed phase, condensed phase with tilted molecules and condensed phase with the untilted molecules on a hexagonal lattice, respectively. The solid lines are drawn based on experimental data, whereas the dashed lines represent the extrapolated phase boundary. The dark region in the right-bottom represents the $L_{2_{SA}}$ phase.

for different mole fractions of DPPC in ChA (X_{PC}) are shown in Figure 3.17. The pure DPPC monolayer [10] shows the liquid expanded ($L_1^{''}$) phase in the range of A_m, 100 to 69 Å^2. It has a plateau representing a coexistence of $L_1^{''}$ and a condensed (L_2) phases in the range of A_m, 69 to 51 Å^2. In the A_m range, 51 - 41 Å^2, it exhibits the L_2 phase. The range of the plateau corresponding to the coexistence of $L_1^{''}$ and L_2 phases of the pure DPPC monolayer decreases due to the presence of ChA in the DPPC monolayer. The isotherm corresponding to X_{PC} equal to 0.9 shows a very small coexisting region of the $L_1^{''}$ and L_2 phases. However, the isotherm corresponding to X_{PC} equal to 0.75 do not show the coexisting region. The isotherms corresponding to X_{PC} less than 0.75 show two kinks indicating two phases. In this X_{PC} range, the surface pressure rises slowly in the beginning and then rapidly till the monolayer collapses. The initial slow varying part shows a large value of extrapolated A_m.

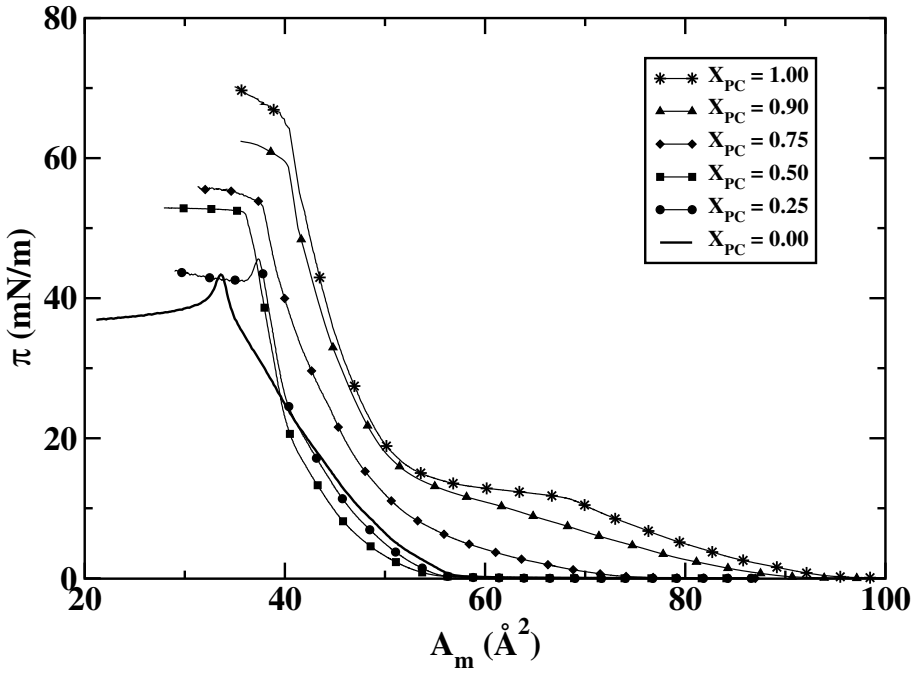

Figure 3.17: The surface pressure (π) - area per molecule (A_m) isotherms of the mixed monolayer for different mole fractions of DPPC in ChA (X_{PC}).

This can be accounted by a tilt of the molecules in the monolayer. The extent of the steep region of the isotherm increases with the increase in X_{PC} indicating a stabilization of the corresponding phase. The limiting area per molecule (A_o) in this region of the isotherm indicates a normal orientation of the molecules at the A-W interface. The variation of collapse pressure (π_c) with respect to X_{PC} is shown in Figure 3.18. The value of π_c for

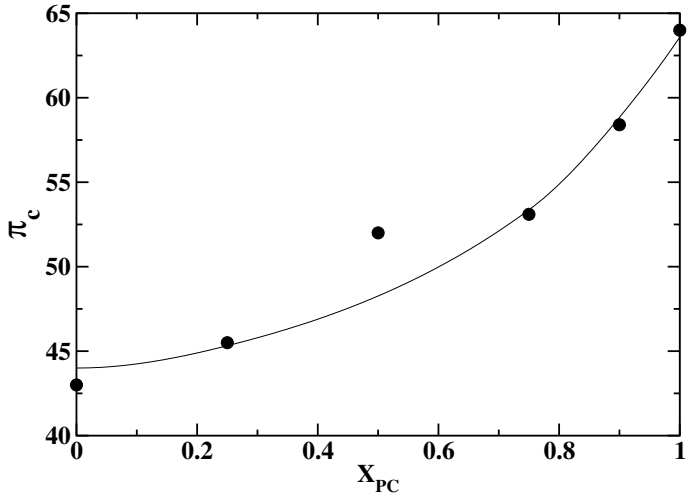

Figure 3.18: Variation of collapse pressure (π_c) with respect to the mole fraction of DPPC in ChA (X_{PC}). The points denote the experimentally obtained data. The solid line is a guide for the eye.

the mixed monolayer system increases continuously with the increase in X_{PC}. This indicates qualitatively a miscible nature of the component molecules in the mixed monolayer [11].

The limiting area per molecule (A_o) values for the isotherms are given in Table 3.3. The A_o values lie in the range of the individual components. This may represent a normal

X_{PC}	0.0	0.25	0.50	0.75	0.90	1.0
A_o (Å^2)	40.8	43.0	42.5	45.0	50.0	50.5

Table 3.3: The limiting area per molecule (A_o) values determined from the isotherms shown in Figure 3.17.

orientation of the molecules in the phase corresponding to the steep rise in surface pressure.

The BAM and epifluorescence images of the pure DPPC monolayer are shown in Figure 3.19. The BAM image of the $L_1^{''}$ phase (Figure 3.19(a)) reveals an uniform gray texture. Figure 3.19(b) shows a coexistence of the $L_1^{''}$ (gray region) and L_2 (bright domain) phases. The epifluorescence image of the $L_1^{''}$ phase reveals an uniform bright region (Figure 3.19(c)). Figure 3.19(d) shows the coexistence of the L_2 phase (dark domains) in the $L_1^{''}$ phase (bright background). The L_2 phase (dark domains) grows on compression. The L_2 domains are dark due to the poor solubility of dye molecules in the L_2 phase of DPPC [12]. The result from microscopy of the DPPC monolayer are consistent with those obtained from the surface manometry studies.

The BAM images of the mixed monolayer for the different X_{PC} are shown in Figure 3.20. The image (Figure 3.20(a)) for X_{PC} equal to 0.25 at a large A_m shows the coexistence of the dark domains (gas phase) and gray regions. On compression, the dark region (gas phase) vanishes and the image (Figure 3.20(b)) shows the uniform gray background. On further compression, the BAM images do not show any change in the texture till the monolayer collapses. The non-appearance of stripe like pattern indicates a suppression of $L_1^{'}$ phase due to the presence of DPPC in ChA monolayer. The BAM image shows (Figure 3.20(b)) the uniform gray texture corresponding to the region of the isotherm which yields a large value of extrapolated A_m. This can be accounted by a tilt of the molecules in the monolayer. Hence, this phase may be considered as the $L_2^{'}$ phase. The image in the steep region of the isotherm

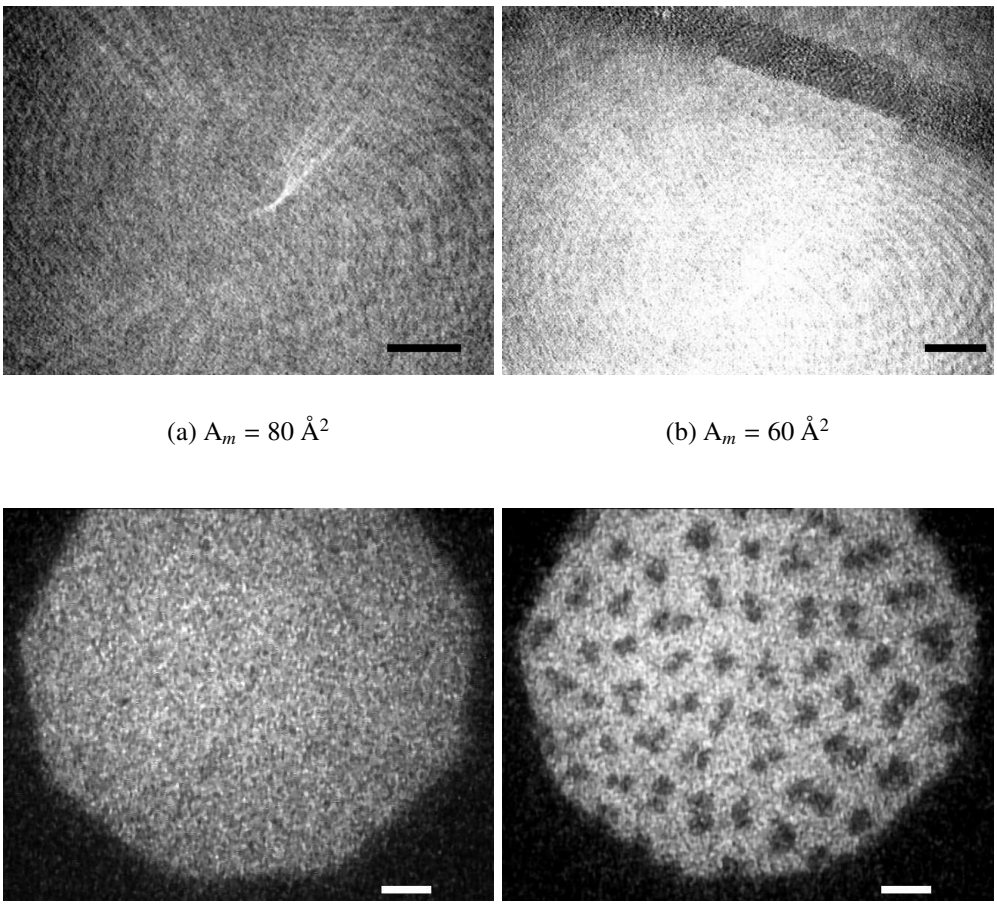

(a) A_m = 80 Å^2 (b) A_m = 60 Å^2

(c) A_m = 85 Å^2 (d) A_m = 64 Å^2

Figure 3.19: (a) and (b) show the BAM images of the pure DPPC monolayer. (a) shows an uniform $L_1^{''}$ phase (uniform gray background). (b) shows a coexistence of $L_1^{''}$ phase (gray region) and L_2 phase (bright background). The BAM images show part of concentric ellipses in the background which are artifacts arising due to scattering of laser light from very fine dust particles on the lens and polarizer of the microscope. (c) and (d) represent epifluorescence images of the DPPC monolayer. (c) shows the uniform gray region which represents $L_1^{''}$ phase. (d) shows the coexistence of $L_1^{''}$ (gray background) and L_2 phase (dark domains). The scale bars in BAM and epifluorescence images represent 500 and 25 μm, respectively.

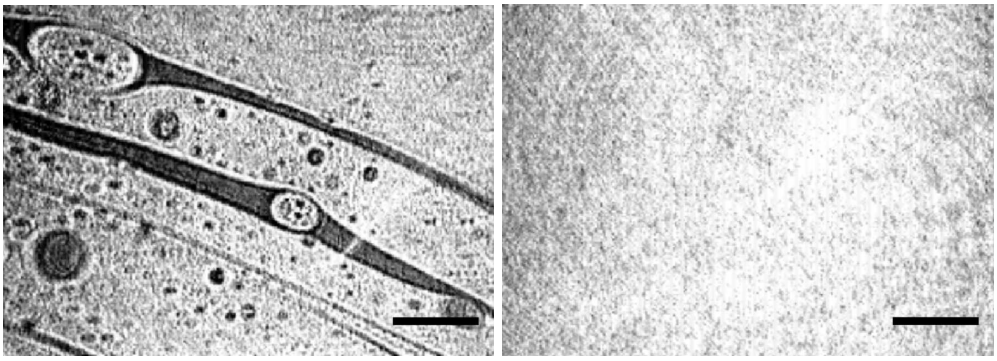

(a) X_{PC} = 0.25, A_m = 67 Å^2 (b) X_{PC} = 0.25, A_m = 45 Å^2

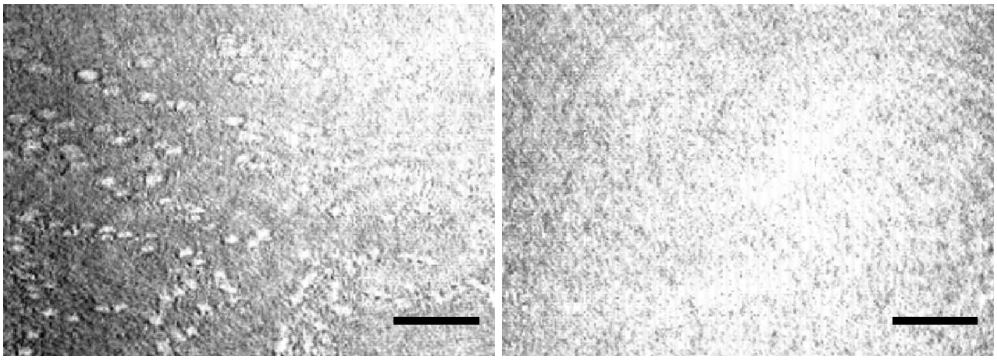

(c) X_{PC} = 0.50, A_m = 41 Å^2 (d) X_{PC} = 0.50, A_m = 37 Å^2

Figure 3.20: BAM images of the mixed monolayer for different mole fractions of DPPC in ChA (X_{PC}). The corresponding mole fraction and the A_m values are shown below the respective images. (a) shows a coexistence of dark region (gas phase) and gray region. (b) shows a very uniform gray texture. (c) shows bright domains growing on a gray background. (d) shows an uniform bright texture. In (b) and (d), part of concentric ellipses in the background are seen. These are artifacts arising due to scattering of laser light from very fine dust particles on the lens and polarizer of the microscope. Such features appear prominently in the images with uniform background. The scale bar represents 500 μm.

also reveals a very uniform gray texture, and the corresponding phase can be considered as the untilted condensed (L_2) phase. The BAM images for the other mole fractions of DPPC in ChA show a similar behavior. However, for the X_{PC} equal to 0.5, we find a coexistence of a few bright domains in a gray uniform background (Figure 3.20(c)). The uniform gray background can be considered as the $L_2^{'}$ phase, whereas the bright domains can be considered as the L_2 phase. On compression, the bright domains grow in size and yield an uniform bright texture (Figure 3.20(d)). The epifluorescence images at a large A_m (Figures 3.21(a) and 3.21(c)) show the coexistence of the gas phase (dark domains) and a liquid-like gray domains. On compression, the monolayer shows an uniform gray background indicating

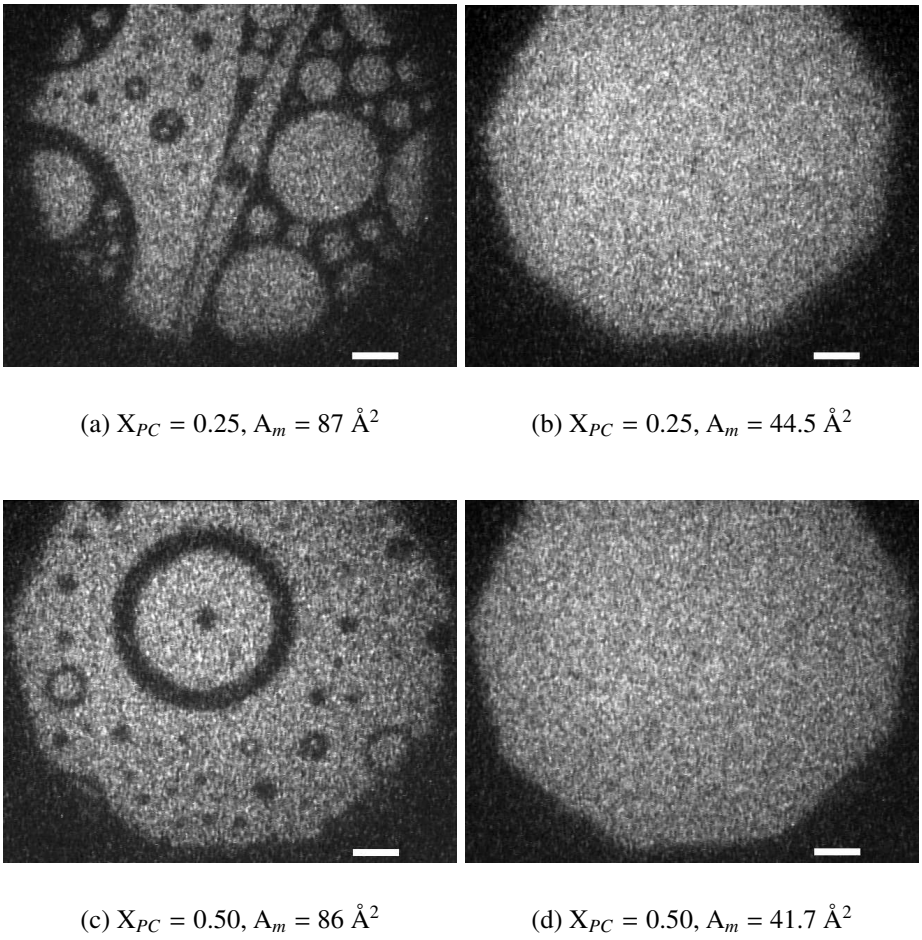

(a) X_{PC} = 0.25, A_m = 87 Å^2 (b) X_{PC} = 0.25, A_m = 44.5 Å^2

(c) X_{PC} = 0.50, A_m = 86 Å^2 (d) X_{PC} = 0.50, A_m = 41.7 Å^2

Figure 3.21: Epifluorescence images of the mixed monolayer for different mole fractions of DPPC in ChA (X_{PC}). The corresponding mole fraction and the A_m values are shown below the respective images. (a) and (c) show a coexistence of dark region (gas phase) and gray domains. (b) and (d) show a very uniform gray texture. The scale bar represents 25 μm.

a homogeneous phase (Figures 3.21(b) and 3.21(d)). The epifluorescence images for the higher concentration of the DPPC show the phases similar to the L_1'' and the L_2 phases.

The variation in the in-plane elastic modulus (E) of the mixed monolayer with A_m for different X_{PC} is shown in Figure 3.22. The variation in E for the pure DPPC monolayer

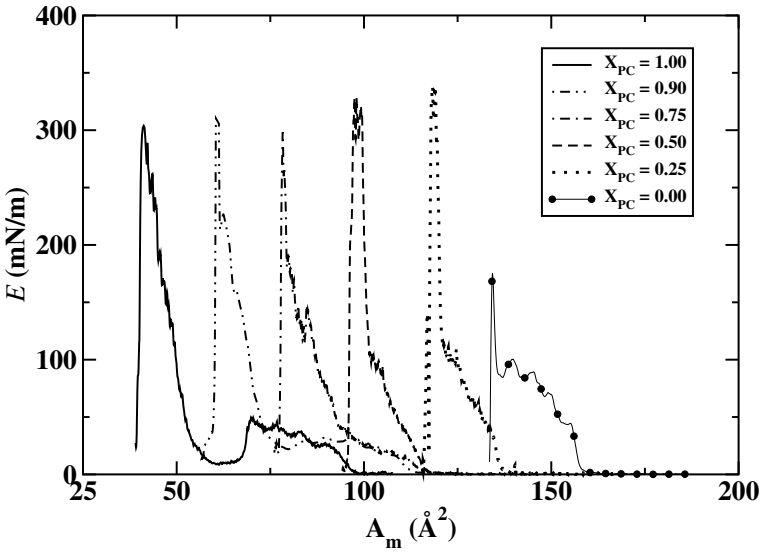

Figure 3.22: Variation of in-plane elastic modulus (E) with respect to the A_m for different mole fractions of DPPC in ChA (X_{PC}). The data presented for the E are smoothened by taking a sliding window of five data points and performing a running average for three times. The curves (except for X_{PC} = 1.0) are relatively shifted horizontally by 20 Å^2 for visual clarity.

shows initially a small rise in the values. This corresponds to the L_1'' phase of the DPPC. Then there is a sharp decrease in E at 68 Å^2 which is quite low upto 58 Å^2. This region corresponds to the coexistence of L_1'' and L_2 phases of DPPC. Then there is a sharp increase in the E value suggesting a phase transition to the L_2 phase. With decrease of X_{PC}, the coexisting region of the L_1'' and L_2 phases disappears. The peak value of E in the L_2 phase remains more or less invariant with the further decrease in X_{PC}. The peak value of E in the L_2 phase of ChA is 175 mN/m which is about 2 times less than that of the mixed monolayer. This indicates that the L_2 phase of the mixed monolayer is more rigid as compared to that of pure ChA monolayer.

The miscibility and the stability of the mixed monolayer for different X_{PC} and at different surface pressures were analyzed by computing the excess Gibbs free energy of the mixed system. The variation of excess area per molecule (A_{ex}) as a function of X_{PC} at different

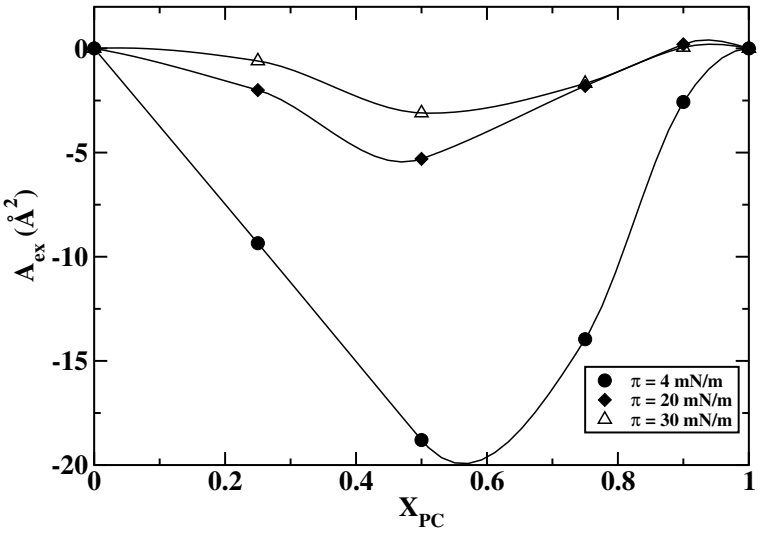

Figure 3.23: The variation of excess area per molecule (A_{ex}) with respect to mole fraction of DPPC in ChA (X_{PC}) at different surface pressures (π). The points denote the calculated values obtained from the experimental data. They are joined by smooth lines.

surface pressures (Figure 3.23) shows negative values suggesting an attractive interaction between the ChA and DPPC molecules in the mixed monolayer. However, $|A_{ex}|$ values decrease with the increase in surface pressure. This indicates that the strength of the attractive interaction between the component molecules reduces with the increase in surface pressure. The variation of the excess Gibbs free energy (ΔG) with respect to X_{PC} at different surface pressures shows negative values for all the compositions (Figure 3.24). The variation shows a minimum at around X_{PC} equal to 0.5 for all the surface pressures. Hence, it can be concluded that the mixed monolayer of the ChA and DPPC are stable for all composition and at all surface pressures. The most stable composition of the mixed monolayer is around 0.5 mole fraction of DPPC in ChA.

Figure 3.25 shows a phase diagram showing the possible the phases of the mixed monolayer of ChA and DPPC.

3.4 Conclusions

We have investigated the miscibility of cholesteric acid with three structurally different molecules. With a similar structure molecule (*i.e.* cholesterol), we find miscibility for all

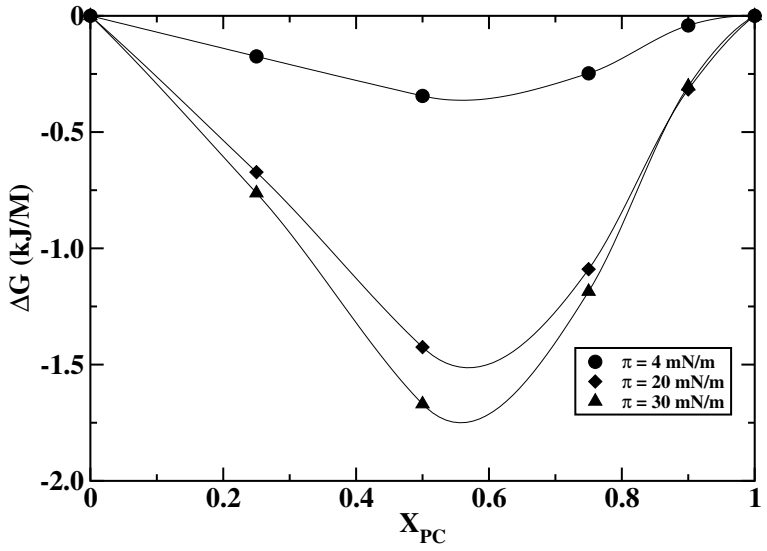

Figure 3.24: The variation of excess Gibbs free energy (ΔG) with different mole fractions of DPPC in ChA (X_{PC}) at different surface pressures (π). The points denote the calculated values obtained from the experimental data. They are joined by smooth lines.

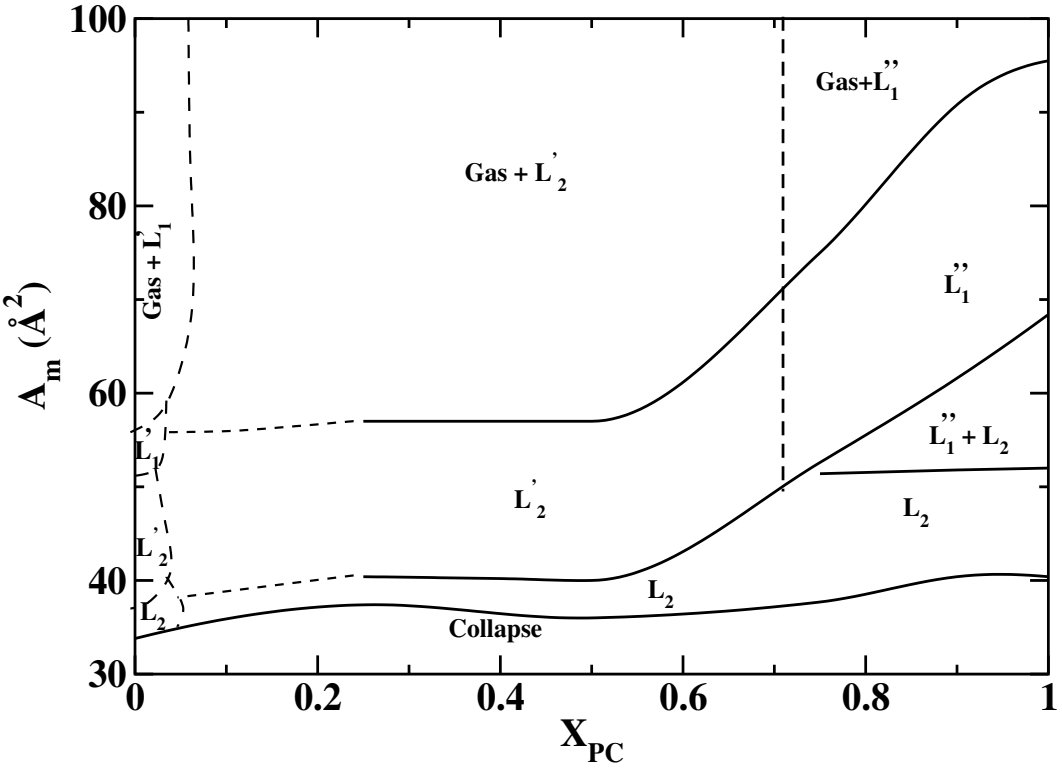

Figure 3.25: Phase diagram of the mixed monolayer of cholesteric acid (ChA) and DPPC. Here, X_{PC} is the mole fraction of DPPC in ChA and A_m is the area per molecule. The symbols $L_1^{'}$, $L_2^{'}$, L_2 and $L_1^{''}$ phases denote a liquid phase with tilt-azimuth varying molecules, a liquid phase with uniformly tilted molecules, untilted condensed phase and liquid expanded phase, respectively. The solid lines are drawn based on experimental data, whereas the dashed lines represent the extrapolated phase boundary.

compositions. These studies show that the tilted $L_1^{'}$ phase get suppressed above 0.5 mole fraction of Ch in ChA. With increasing mole fraction of Ch in ChA, the extent of the $L_2^{'}$ phase reduces, whereas the L_2 phase stabilizes. In the monolayer of pure Ch, the molecules assemble to yield an untilted condensed (L_2) phase. Such orientation of the Ch molecules induces an effect which leads to the stabilization of the L_2 phase of the mixed monolayer. The Ch molecule shows an attractive interaction with the ChA molecule in the mixed monolayer. Such attractive interaction can arise due to the van der Waals and hydrophobic interactions between the sterol moiety of the molecules and the ease of formation of hydrogen bond of the head groups of ChA and Ch with the water molecules. Our study on the mixed monolayer of a linear molecule possessing an alkyl chain (stearic acid) and ChA indicates a partial miscibility. We find a miscible monolayer only at X_{SA} equal to 0.4. The immiscibility of the molecules can be attributed to the difference in shapes of the molecules. However, the loosely packed ChA molecules in the monolayer may accommodate few SA molecules without any appreciable reduction in entropy of the system. This may lead to a partial miscible nature of the components. A bulkier molecule (DPPC) possessing two aliphatic tails and a large head group mixes readily in the ChA monolayer. The study shows that the X_{PC} equal to 0.5 is the most stable composition. The presence of DPPC in ChA suppresses the $L_1^{'}$ phase.

Bibliography

[1] N. A. Nelson, R. C. Kelly, and R. A. Johnson, Chem. Engg. News **60**, 30 (1982).

[2] R. Ross, Nature (London) **362**, 801 (1993).

[3] R. Lipowsky and E. Sackmann, *Handbook of Biological Physics* (Elsevier Science,Amsterdam, 1995) Chapter 4.

[4] S. Lafont, H. Rapaport, G.J. Sömjen, A. Renault, P.B. Howes, K. Kjaer, J. Als-Nielsen, L. Leiserowitz, and M. Lahav, J. Phys. Chem. B **102**, 761 (1998).

[5] J. P. Slotte and P. Mattjus, Biochim. Biophys. Acta **1254**, 22 (1995).

[6] F. C. Goodrich, in *Proceedings of the 2nd International Congress on Surface Activity*, edited by J. H. Schulman (Butterworths, London, 1957), Vol. 1, P. 85.

[7] R. Seoane, P. Dynarowicz-tstka, J. Miñones Jr., and I. Rey-Gòmez-Serranillos, Colloid Polym. Sci. **279**, 562 (2001).

[8] P. Viswanath and K. A. Suresh, Phys. Rev. E **67**, 061604 (2003).

[9] V. M. Kaganer, H. Möhwald, and P. Dutta, Rev. Mod. Phys. **71**, 779 (1999).

[10] K. S. Birdi, *Lipid and Biopolymer Monolayers at Liquid Interfaces* (Plenum, New York, 1989).

[11] G. L. Gaines Jr. *Insoluble Monolayers at Liquid-Gas Interfaces* (Wiley-Interscience, New York, 1966).

[12] R. M. Weis and H. M. McConnell, Nature (London) **310**, 47 (1984).